The long term indoor atmospheric corrosion of iron: rust layer characterisation

Judith Monnier, Ludovic Bellot-Gurlet, Ludovic Legrand, Philippe Dillmann, Solenn Reguer, Delphine D. Neff, Ivan Guillot

The long term indoor atmospheric corrosion of iron: rust layer characterisation

Judith Monnier[a,b], Ludovic Bellot-Gurlet[c], Ludovic Legrand[d], Philippe Dillmann[a,e], Solenn Reguer[f], Delphine Neff[a] and Ivan Guillot[b]*

[a] Laboratoire Pierre Süe (LPS), UMR 9956 CEA/CNRS, bât. 637 CEA Saclay 91191 Gif-sur-Yvette, France
[b] Institut de Chimie et Matériaux Paris-Est (ICMPE) UMR 7182, 2-8, rue H. Dunant, 94320 Thiais, France
[c] Laboratoire de Dynamique, Interaction et Réactivité (LADIR), UMR 7075, 2-8, rue H. Dunant, 94320 Thiais, France
[d] Laboratoire Analyse et Modélisation pour la Biologie et l'Environnement (LAMBE), UMR 8587, Évry, France
[e] Laboratoire Métallurgies et Cultures (LMC) UMR 5060, Belfort, France
[f] Synchrotron SOLEIL, Saint-Aubin BP 4891192 Gif-sur-Yvette, France

* Corresponding author: judith.monnier@cea.fr

Abstract

The study of long term indoor atmospheric corrosion is involved in the field of iron bearing in building heritage. Concerning historical artefacts, due to the complexity of the system, it is necessary to couple many analytical techniques from the macro to the microscopic scale. This enables a schematisation of the Amiens cathedral chains rust layer, constituted of a matrix of goethite, with lepidocrocite locally present in the rust layer and marblings of a poor crystallised phase associated to ferrihydrite. The reduction capacity of the rust layer has also been studied using electrochemical methods.

Keywords: ancient iron artefacts, indoor atmospheric corrosion, coupled analytical techniques

Introduction

Numerous ancient monuments contain high quantities of iron reinforcement in their structure. These rods and clamps have been put in the building during their construction or for later reinforcement (L'Héritier 2004; L'Héritier et al. 2005; Dillmann and L'Héritier in press). Many of these iron alloy reinforcement are submitted to atmospheric corrosion for several hundred years and the behaviour of these heritage metallic materials has to be predicted for conservation and restoration reasons. Moreover, in museum collections or in industrial heritage, a lot of artefacts are constituted of non painted iron alloys that have to be protected from corrosion. In this context, questions still remain about the very long term corrosion mechanisms. In fact, laboratory tests enable to model the corrosion behaviour for a few ten years, but are inefficient for longer periods. Indeed, the final aim of the study presented here is to propose a diagnosis method that could be applied to evaluate the reactivity degree of the layer and consequently the corrosion rate. This method will be based on the one hand on electrochemical studies of the phases present in the old corrosion layers and, on the other hand on their fine structural characterisation. To these purpose, ancient samples submitted to multisecular indoor atmospheric corrosion are studied in order to enlighten the very long term corrosion mechanisms.

The first part of this paper will be dedicated to a short literature review that will expose the atmospheric corrosion mechanisms commonly found in literature and based on the wet/dry cycle. It will be shown that some constitutive phases of the corrosion layer can act in the corrosion processes of iron, controlling the corrosion rates. That is why, after a paragraph dedicated to sample and analytical methods description, the fine characterisation results of ancient rust layers will be presented. These results are then completed by an electrochemical study of the ancient corrosion layer.

Literature review on atmospheric corrosion

Atmospheric corrosion is controlled by the so-called "wet-dry" cycle (Evans and Taylor 1972). Depending on the relative humidity (RH) of the atmosphere, a water film will condensate, on the surface of the iron. The combined presence of an oxidant, an electrolyte and the metal provokes corrosion processes. The rust formed has in reality a complex composition. From literature data, the main phases in rust are goethite (α-FeOOH), lepidocrocite (γ-FeOOH), maghemite (γ-Fe_2O_3) and magnetite (Fe_3O_4) (Dillmann et al. 2004). These crystallised phases can easily be identified in the corrosion products by X-ray diffraction (XRD) and μXRD methods. More recently, using μ-Raman spectroscopy, less crystallised phases have been detected: feroxyhite (δ-FeOOH) and/or a type of ferrihydrite, a hydrated oxyhydroxide that can be present under two forms according to literature (Misawa et al. 1974; Neff et al. 2006).

In the first stage of the wet-dry cycle (see figure 1), the "wetting stage", the water film forms at the surface of the sample. During this step, it can be showed that iron consumption is

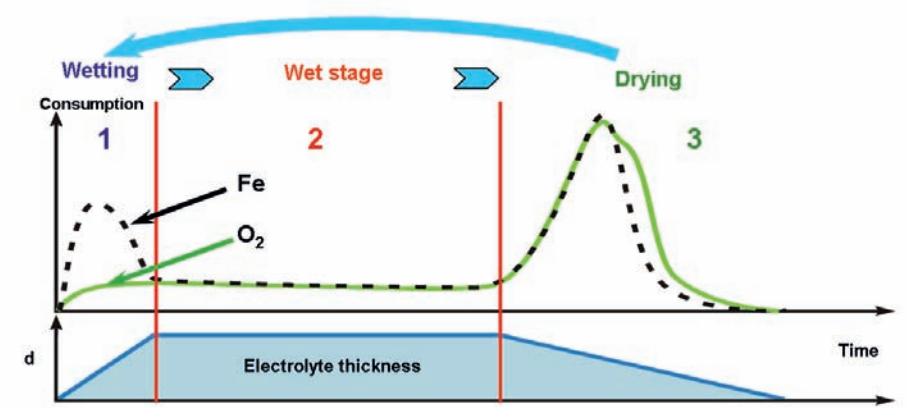

Figure 1: Wet-dry cycle taking place during atmospheric corrosion

much higher than oxygen one (Stratmann et Streckel 1990). But, to observe the oxidation-reduction reaction causing iron consumption, another phase of the system should be reduced. Experiments made on rusted iron coupons proved that the rust layer contains one (or more) phases which are reactive and able to be reduced, and act in the corrosion processes. Moreover, some recent electrochemical studies (Lair et al. 2006) point out the reduction capability of different oxide phases and enable the following reduction activity ranking:

Magnetite << Goethite ≈ maghemite < Lepidocrocite < Ferrihydrite ≈ Feroxyhite

Therefore some phases in the corrosion layer can be defined as active ones and others as stable. A ratio has thus been proposed between potential active and non active phases. Depending on the authors, different phases are considered to define this α/γ stability ratio (see table 1). This point is not so far clear and some important phases as ferrihydrite and/or feroxyhite have not been considered up to now.

As a consequence, two research axes are defined here. First, a fine characterization of the corrosion layer has to be made, in order to confirm what phases are present in the rust layer. Secondly, the electrochemical behaviour of the corrosion layer itself has to be studied in correlation with reference phase reactivity. To this purpose, it was chosen to focus in a first step on one single site where numerous specimens can be sampled.

Site of the study and experimental methods

Site of the study

All the studied samples are coming from the Amiens cathedral chain. This cathedral was built in the 13th century, but in 1498 a reinforcement chain made of iron bars was put all around the Triforium (Lefebvre 2006) as can be seen on figure 2. The chain is constituted of 90 bars of 4 m long. It was possible to sample 58 specimens of about 1 cm^3 all around the Triforium. Up to now, 25 have already been analysed. Temperature (T) and relative humidity (RH) data loggers (Kistock, KIMO Constructeur) were put at different places, (see figure 2c) of the building near the irons bars.

Analytical methods

Representative parts of the corrosion system were sampled on the iron bars. Samples are first mounted into cross sections in Mecaprex MA2 epoxy resin. They are ground with SiC abrasive papers (grades 800 to 4000) then using diamond paste (3 and 1 μm) under ethanol.

μ-XRD analyses (see below) need a specific sample preparation under thin films. Cross-sections are pasted on glass slides with a balsam soluble in acetone only. By polishing with SiC papers under ethanol, samples thickness is reduced to approximately 100 μm (Réguer et al. in press).

First observations are performed using an optical microscope to obtain a general overview of the corrosion layout. Chemical composition of the rust layers follows then by energy dispersive spectrometry (EDS) (SAMx IDFix software) coupled to a scanning electron microscope (SEM) (LEO 120, Cambridge Instruments, operating at 15 kV). The Si(Li) detector used for these EDS analyses is equipped with a thin beryllium window in order to detect and quantify oxygen with a good accuracy (about 2wt% relative error on iron oxides standards).

In order to identify and localise the crystallised phases present in the rust layer previous studies have shown that the coupling of μ-Raman spectrometry and μ-XRD is very efficient (Neff et

Table 1: Definition of the stability ratio α/γ

Author	Ratio definition
(Yamashita et al. 1994)	α/γ, α=goethite wt% ; γ=lepidocrocite wt%
(Kihira et al. 1999)	(α + am)/γ*, am=amorphous phases detected with XRD technique; γ*=β-FeOOH + γ-FeOOH + Fe_3O_4
(Kashima et al. 2000)	α/γ*, α=α-FeOOH and γ*=γ-FeOOH + β-FeOOH + Fe_3O_4
(Dillmann et al. 2004)	α*/γ*, α*=α-FeOOH + Fe_3O_4 and γ*=β-FeOOH + γ-FeOOH

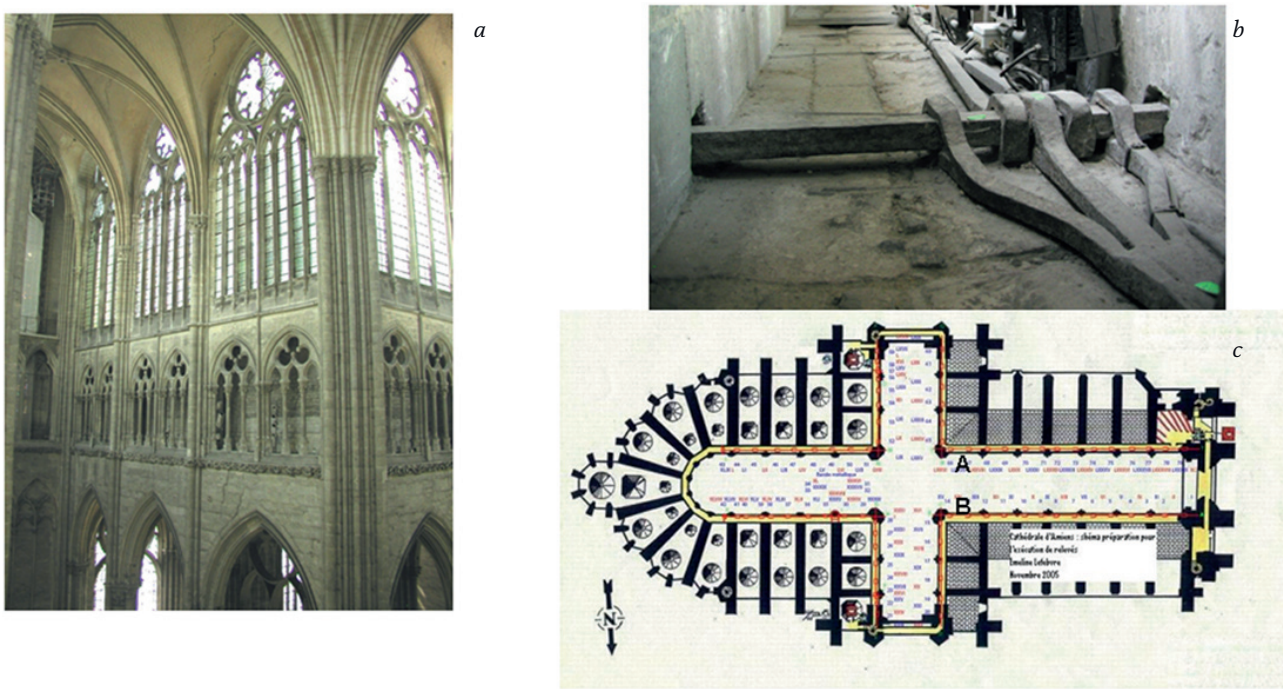

Figure 2: Amiens cathedral; (a) Triforium photograph; (b) Iron chains bar placed around the Triforium; (c) Cathedral map, with T/RH detectors placements (A and B points)

al. 2006). µ-Raman measurements were performed at LADIR with a micro-Raman Notch-based spectrometer LabRam Infinity (Jobin Yvon-Horiba) using a laser radiation at 532 nm. Samples were observed under an Olympus microscope with Leitz objectives 100x, giving a beam waist diameter of about 3µm. The spectrometer setting offers a spectral resolution of about 2 cm^{-1}. As some iron oxides are highly sensitive to laser irradiation (de Faria et al. 1997), measurements are always performed with a power on the sample below 100 µW in order to avoid any phase transformation. Spectra identification is done by comparison with reference spectra (Neff et al. 2006).

X-ray micro diffraction (µXRD) analyses were performed on the photon microprobe developed in common by the LPS and the LMC. This microprobe is built on a rotating anode X-ray generator. The beam delivered by a Molybdenum (K_α at 17.45 keV) anode is monochromatised and concentrated on a surface of 20 x 20 μm^2 by a torroïdal mirror and a borosilicate capillary. µXRD patterns are collected in transmission mode downstream a thin film sample by a 2D image plate detector.

Because several phases that could be present in the rust layers and involved in the corrosion mechanisms of iron are poorly crystallised, it is necessary to perform specific microprobe methods to find them in the corrosion scales. One of the most efficient one is the µ-X-ray absorption spectrometry (µXAS). This method, because of the fine energy resolution it needs, must be performed using synchrotron radiation. For the present study, µ-XAS experiments were performed on LUCIA beamline at Swiss Light Source. The energy scans were performed using a fixed exit silicon Si(110) double crystal monochromator. The synchrotron X-ray source was focused to a 3x4.5 μm^2 beam. Series of XAS spectra were collected in fluorescence mode, from 7050 to 7800 eV at the Fe K-edge. A metallic Fe foil is used to provide internal energy calibration of the monochromator. Moreover, XAS spectra were also acquired on oxide and oxyhydroxide reference powders.

Electrochemical measurements are made at LAMBE in a three electrodes cell. Reference electrode is an AgCl coated silver wire; the counter one is a platinum electrode. For the working electrode a composite electrode made of graphite powder mixed with the sample powder compressed on a stainless steel grid was used. Samples consist of Amiens chains rust powder. The electrolyte used is a deaerated NaCl 0.1 M solution, with buffered pH at 7.5 (PIPES solution, 0.05 M). Temperature is controlled and fixed at 25°C. Intentiostatic curves are recorded by imposing 25 µA/mg matter.

Results and discussion

Temperature and RH measurements

The obtained results show that at the two detector locations, the temperature and RH signals are very similar, as can be seen in figure 3a. That could be explained by the fact that the two detectors are placed in the cathedral nave, where the air drafts are maybe the most important. As a consequence, we consider only one detector the following comparison with METEO France data collected on Glisy airport near Amiens. During months of exposures, daily variations of relative humidity and temperature are strongly dumped inside the cathedral with respect to outside (METEO France values). Monthly temperature variation is also smoother inside than outside, even though the overall excursion on the six months considered is almost the same (see figure 3b and table 2). For the relative humidity, instead of very well defined daily wet-dry cycles outside, two types of variation have to be noticed near iron chains. Daily cycles could be evidenced but with less amplitude than outside

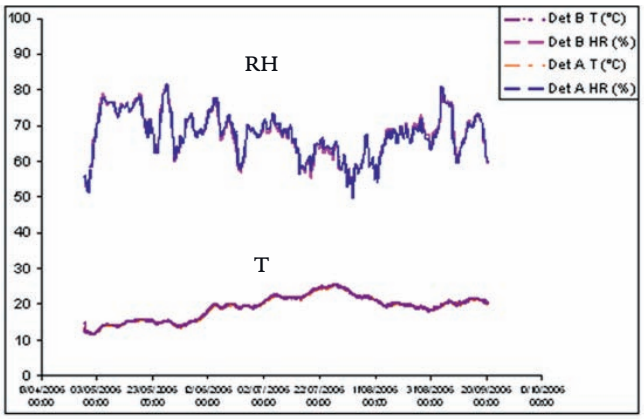

Figure 3: Temperature and relative humidity detectors on Amiens cathedral chain; (a) detectors A and B measurements comparison; (b) Detector A and METEO France data comparison for May to August 2006

a/

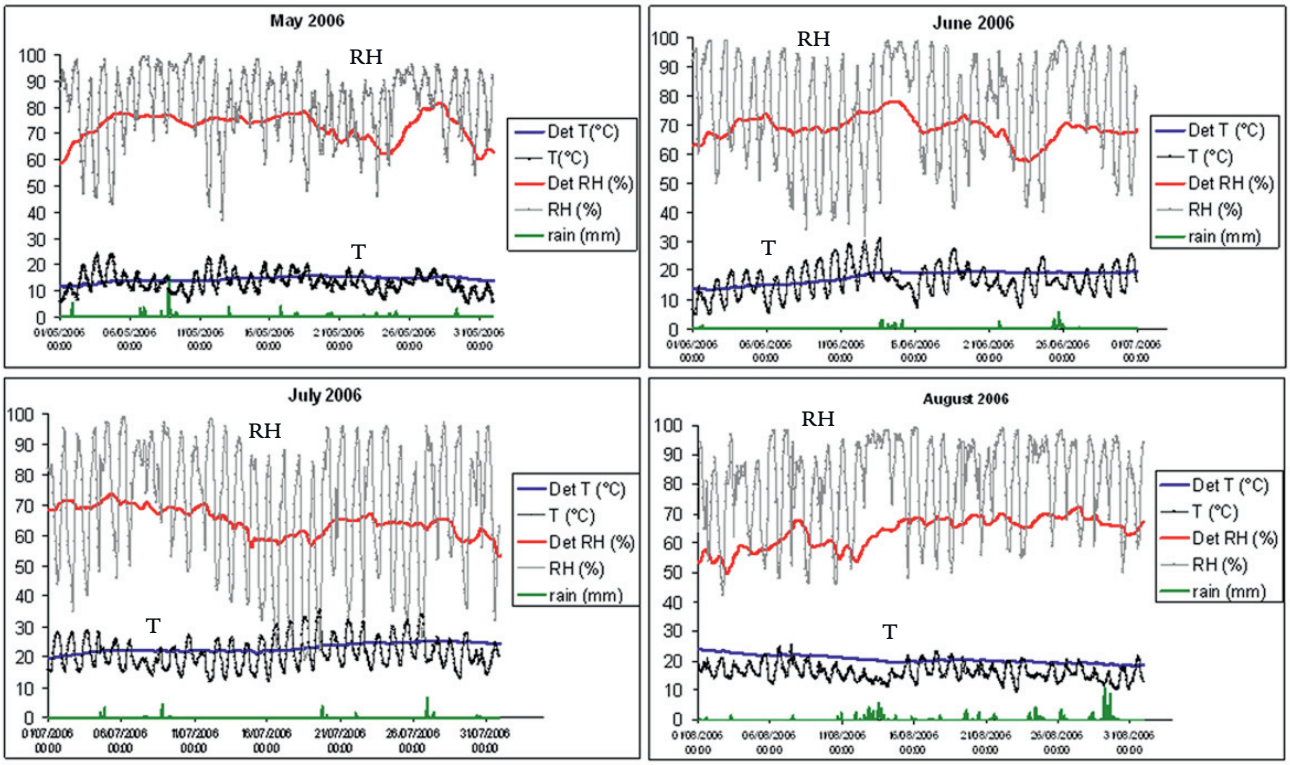

b/

Table 2: Minima and Maxima Temperature and Relative Humidity recorded in Amiens cathedral compared to Glisy airport data

	T min		T max		RH min		RH max	
	MF data	detector	MF data	detector	MF data	detector	MF data	detector
April 06	1,1	11,56	15	13,99	33	51,3	97	58,9
May 06	5,3	11,58	24,4	15,88	35	58,5	100	81,5
June 06	4,5	13,31	31,1	19,96	31	57,3	99	77,9
July 06	11,4	19,8	36	25,21	17	52,9	99	73,6
August 06	9,4	18,45	25,3	24,22	39	49,6	99	72,2
September 06	6,8	18,58	28,9	21,87	31	59,4	99	81,2

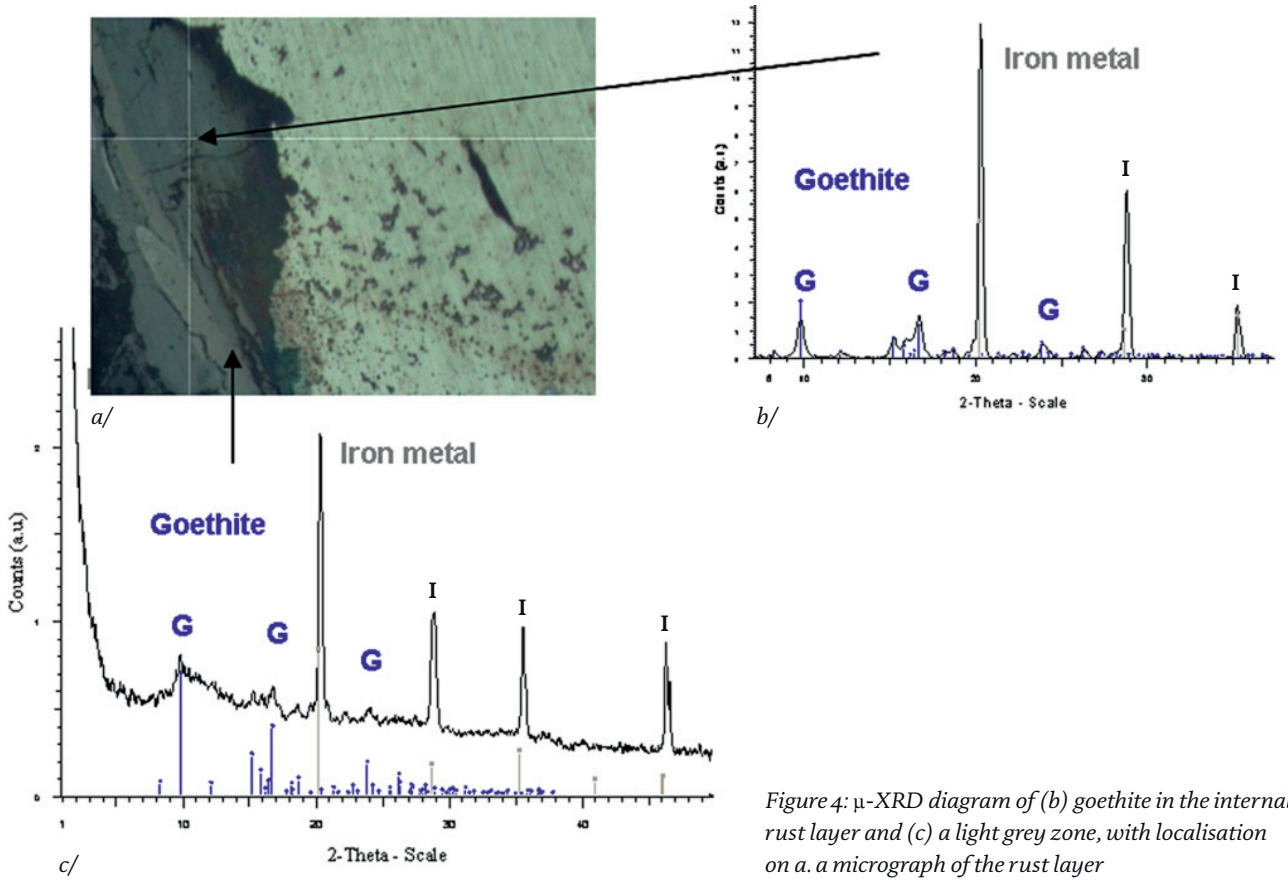

Figure 4: µ-XRD diagram of (b) goethite in the internal rust layer and (c) a light grey zone, with localisation on a. a micrograph of the rust layer

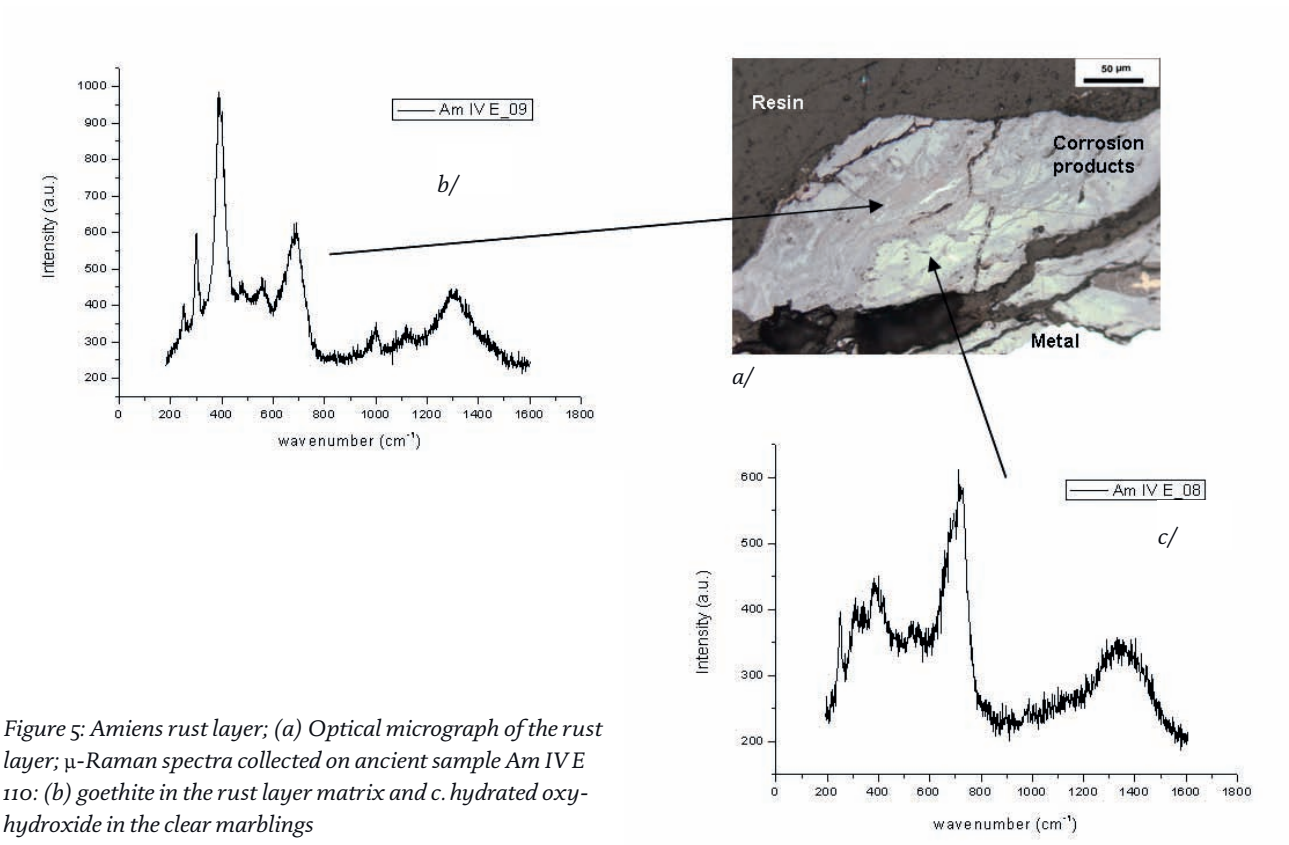

Figure 5: Amiens rust layer; (a) Optical micrograph of the rust layer; µ-Raman spectra collected on ancient sample Am IV E 110: (b) goethite in the rust layer matrix and c. hydrated oxy-hydroxide in the clear marblings

and cyclic variations due to deep changes in weather should be added to these "minor daily cycles". Rain does not seem to act directly on inside relative humidity.

Physico-chemical analysis on historical artefacts

Historical samples have been studied on transverse section using an optical microscope first, then μ-XRD, SEM and μ-Raman spectroscopy. The average thickness of the corrosion layer is around 100 μm (see figure 5a). Some cracks are present. Very large ones, parallel to the metal/oxide interface could have been made during sampling. But cracks are also due to the rust layer growing. The layer is constituted of a dark grey matrix in which some light grey zones are visible; they can sometimes be in contact with the metal core, but more often are dispersed in the more or less uniform rust layer. EDS analyses reveal, in addition to Fe and O, the presence of impurities in the rust layer. The local presence of calcium can be correlated with calcite coming from the walls.

μ-XRD (see figure 4) and μRaman (see figure 5) analyses reveal the presence of goethite α-FeOOH as the most common phase in the rust layer. Lepidocrocite γ-FeOOH is also present, but much more locally and more in the external zone of the corrosion layer. Akaganeite β-FeOOH, an iron oxy-hydroxide containing chlorides in its structure is detected on 11 samples under 17 analysed, in very localised spots near cracks or in the external zone of the rust layer. Its presence could be correlated to chlorides in the electrolyte layer. In addition to the identification and localisation of well crystallised phases, analyses conducted with μ-Raman spectroscopy, giving a smaller beam than μXRD, also permit to identify other localised phases. On spectra collected in lighter zones of the corrosion layer (Figure 5c) a wide band around 700 cm^{-1} is recorded. By comparison with reference spectra made on synthesised powders, they could be assimilated to 3 types of phases: a maghemite, a poor crystallised feroxyhite or a ferrihydrite. All these phases present a broad peak around these wave number, thus it is tricky to distinguish it only using μRaman spectroscopy. Yet, literature proves that these phases can have very different reactivity. Thus, it is of primary importance to try to distinguish them in the corrosion product.

For this reason μXAS spectra were collected at the Fe K-edge in the light grey zones of the corrosion layers. The reference spectra show that EXAFS signal is convenient to distinguish the different phases (see figure 6). On a historical sample, the spectra obtained seem to fit ferrihydrite phase spectra.

Thus, it can be concluded that chemical and structural analyses reveal the same general morphology of the rust layer for all samples: a matrix composed of goethite with other phases locally present, lepidocrocite, akaganeite and what seems to be a type of ferrihydrite, as is presented on figure 7. As Ferrihydrite presence is confirmed, the α/γ ratio established in literature has to be refined.

Electrochemical study of ancient rust layers

In order to complete the electrochemical study on reference phases, the reduction reactivity of the rust layer was investigated and compared to the results already obtained for such samples by Antony (2005). Through the potential versus time curves we can extract a reactivity ratio, which measures the reduction capability of the rust layer. Values obtained for Amiens cathedral are placed on an existing graph, and are in good agreement with Antony's measurements. The reactivity ratio versus age curve (see figure 8) points out a decrease of the reactivity ratio with the age of the samples. As a consequence,

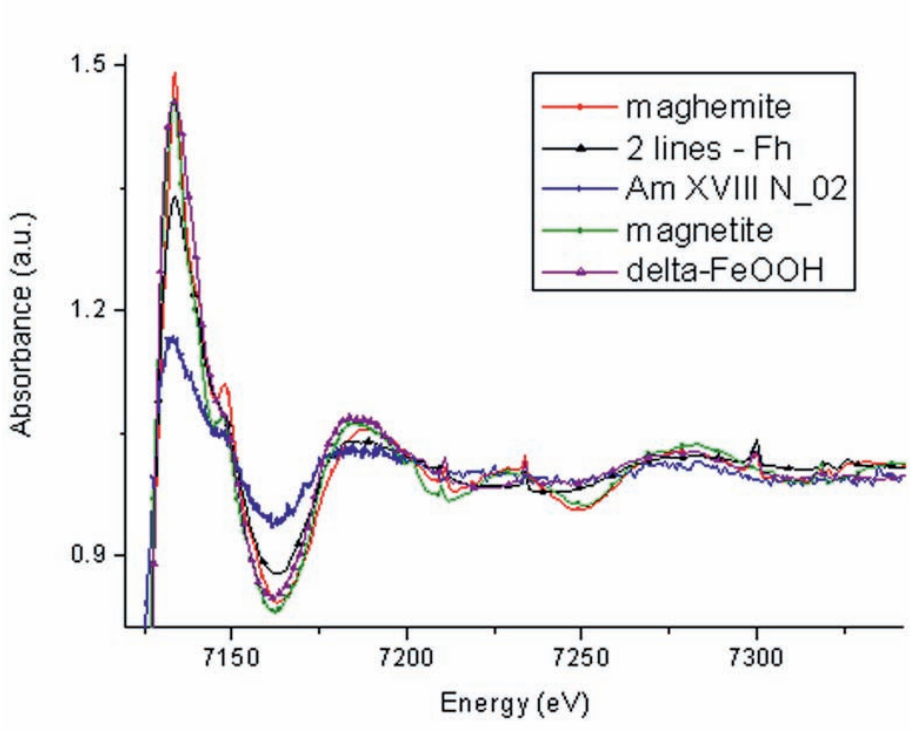

Figure 6: EXAFS raw signals of references phase compared with an experimental spectrum on Am XVIII N

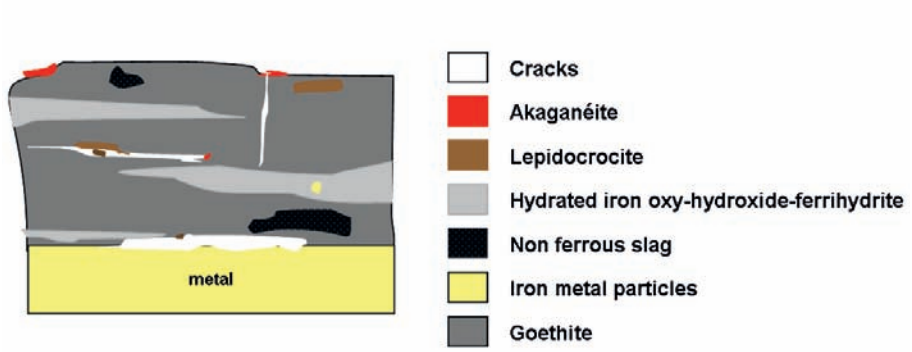

Figure 7: Schematic view of the corrosion layer developed on the Amiens iron chains

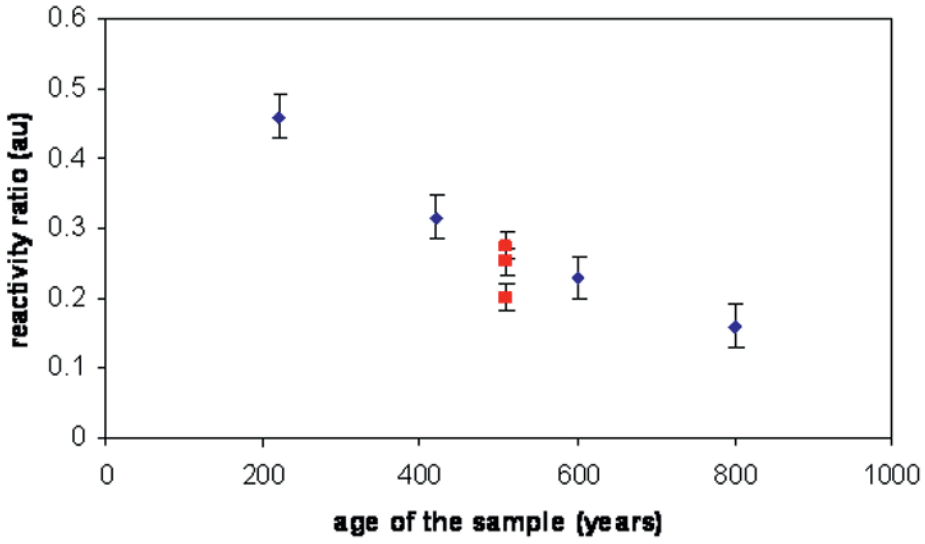

Figure 8: Reactivity ratio evolution versus sample age; Antony (2005) (rhomb), this study (square)

we could propose to replace or refine the stability ratio existing in literature and based on characterisation data by the reactivity ratio defined here based on electrochemical measurements.

Conclusion

Several samples coming from a reference site for indoor atmospheric corrosion have been characterised using coupling between micro-focused techniques. A schematic view of the corrosion layer can be drawn, with a goethite matrix crossed by hydrated iron oxy-hydroxide marblings. Lepidocrocite is detected in locally places, as well as akaganeite. As a consequence, the α/γ stability ratio defined in literature should be refined, maybe taking into account the reactivity ratio established through electrochemical measurements. This could enable conservation communities to build a reactivity diagnosis for iron historical artefacts.

Acknowledgements

The authors would like to thank the architects, historians and archaeologists who supplied the samples and contributed to this study, and particularly Maxime L'Heritier (LPS), Arnaud Thimbert (Université Lille1) and Ms Emeline Lefebvre (Université Lille1), Eddy Foy and Delphine Vantelon for their precious help in respectively μ-XRD and μ-XAS analyses.
This work is founded by the French program ANR ARCOR, the GdR Chim'Art and the PNRC "Corrosion Atmosphérique" of French Ministère de la Culture.

References

- Antony H. 2005. Etude électrochimique des composés du fer - Apport à la compréhension des processus environnementaux. Thesis, Evry, France
- de Faria D.L.A., S.V. Silva and M.T.d. Oliveira. 1997. Raman micro spectroscopy of some iron oxides and oxyhydroxides, Journal of Raman Spectroscopy, 28, 873-878
- Dillmann P., F. Mazaudier and S. Hoerle. 2004. Advances in understanding atmospheric corrosion of iron I - Rust characterisation of ancient ferrous artefacts exposed to indoor atmospheric corrosion, Corrosion Science, 46(6), 1401-1429
- Dillmann P. and M. L'Héritier, In press. Slag inclusion analyses for studying ferrous alloys employed in French medieval buildings: supply of materials and diffusion of smelting processes, Journal of Archaeological Science
- Evans U.R. and C.A.J. Taylor. 1972. Mechanism of Atmospheric Rusting, Corrosion Science, 12(3), 227-246
- Kashima K., S. Hara, H. Kishikawa and H. Miyuki. 2000. Evaluation of protective ability of rust layers on weathering steels by

potential measurement, Corrosion Engineering, 49(1), 25-37
- Kihira H., T. Misawa, T. Kusunoki, K. Tanabe and T. Saito. 1999. How to use the composition ratio index obtained by internal standard quantitative X-Ray diffraction Analysis to evaluate the state of rust on weathering steel, Corrosion Engineering, 48, 979-987
- L'Héritier M. 2004. L'utilisation du fer à la cathédrale de Rouen à l'époque médiévale. Haute Normandie Archéologique, Eu, CRAHN
- L'Héritier M., A. Juhin, P. Dillmann, R. Aranda and P. Benoit. 2005. Utilisation des alliages ferreux dans la construction monumentale du Moyen Age. État des lieux de l'avancée des études métallographiques et archéométriques, La Revue d'Archéométrie, 29, 117-132
- Lair V., H. Antony, L. Legrand and A. Chausse. 2006. Electrochemical reduction of ferric corrosion products and evaluation of galvanic coupling with iron, Corrosion Science, 48, 2050-2063
- Lefebvre E. 2006. La place et le rôle des métaux dans l'architecture gothique à travers l'exemple de la cathédrale d'Amiens. Étude de cas : le chaînage du triforium de la cathédrale d'Amiens, Amiens
- Misawa T., K. Asami, K. Hashimoto and S. Shimodaira. 1974. The mechanism of atmospheric rusting and the protective amorphous rust on low alloy steel, Corrosion Science, 14, 279-289
- Neff D., L. Bellot-Gurlet, P. Dillmann, S. Reguer and L. Legrand. 2006. Raman imaging of ancient rust scales on archaeological iron artefacts for long term atmospheric corrosion mechanisms study, Journal of Raman Spectroscopy, 37, 1228-1237
- Réguer S., P. Dillmann and F. Mirambet, In press. Buried iron archaeological artefacts: corrosion mechanisms related to the presence of Cl-containing phases, Corrosion Science
- Stratmann M. and H. Streckel. 1990. On the atmospheric corrosion of metals which are covered with thin electrolyte layers - II. experimental results, Corrosion Science, 30(6/7), 697-714
- Yamashita M., H. Miyuki, Y. Matsuda, H. Nagano and T. Misawa. 1994. The long term growth of the protective rust layer formed on weathering steel by atmospheric corrosion during a quarter of a century, Corrosion Science, 36(2), 283-299